https://doi.org/10.5194/gmd-2021-129
Preprint. Discussion started: 17 May 2021

Geoscientific Model Development
Discussions

Particle dry deposition algorithms in CMAQ version 5.3: characterization of critical parameters and land use dependence using DepoBoxTool version 1.0

Qian Shu[1], Benjamin Murphy[1], Jonathan E. Pleim[1], Donna Schwede[1], Barron H. Henderson[2], Havala O.T. Pye[1], Keith Wyat Appel[1], Tanvir R. Khan[3*], Judith A. Perlinger[3]

[1] The Center for Environmental Measurement and Modeling, U.S. Environmental Protection Agency, Research Triangle Park, NC 27711, USA.
[2] Office of Air Quality Planning and Standards, U.S. Environmental Protection Agency, Research Triangle Park, NC, 27711, USA.
[3] Department of Civil and Environmental Engineering, Michigan Technological University, Houghton, MI 49931, USA.
* now with: FSEC Energy Research Center, University of Central Florida, Cocoa, 32922, USA.

Correspondence to: Qian Shu (shumarkq@gmail.com)

Abstract. This study investigates particle dry deposition by characterizing critical parameters and land-use dependence in a 0-D box model as well as quantifying the resulting impact of dry deposition parameterizations on regional-scale 3-D model predictions. A publicly available box model (DepoBoxToolv1.0) configured with several land-use dependent dry deposition schemes is developed to evaluate predictions of several model approaches with available measurements. The 0-D box model results suggest that current dry deposition schemes in 3-D regional models underestimate particle dry deposition velocities, but this varies with size distribution properties and land-use categories. We propose two revised schemes to improve dry deposition performance in air quality models and test them in the Community Multiscale Air Quality (CMAQ) model. The first scheme improves the previous CMAQ scheme by preserving the original dry deposition impaction calculation but turning off redundant integration across particle size for each aerosol mode. The second scheme adds a dependence on leaf area index (LAI) to better estimate uptake to vegetative surfaces while using a settling velocity that is integrated across particle size for the Stokes number calculation. CMAQ model performance was evaluated for a month in July 2011 for the conterminous U.S. based on available observations of ambient sulfate (SO_4^{2-}) aerosol concentrations from multiple routine particulate matter monitoring networks. Incorporation of the first scheme has a larger impact on coarse particles than fine particles, systematically reducing monthly domain-wide average particle dry deposition velocities (V_d) by approximately 96% and 35%, respectively, and increasing monthly average SO_4 concentrations by 395% and 21%. After incorporating LAI into the boundary layer resistance (R_b), the second scheme creates more spatial diversity of V_d and changes SO_4 concentrations (coarse = -76% to +336%; fine = -7% to +18%) with land-use categories. These modifications are incorporated into the current publicly available version of CMAQ (v5.3 and beyond).

1 Introduction

Dry deposition is an essential removal process for atmospheric particles and can account for a significant fraction, sometimes more than half, of the total deposition of many important chemical compounds in the

https://doi.org/10.5194/gmd-2021-129
Preprint. Discussion started: 17 May 2021

atmosphere (Lovett, 1994). The ability of atmospheric models to represent dry deposition processes directly affects the skill with which they can predict particle concentrations with implications for radiative forcing and the role of particles in climate change (Emerson et al., 2020). A previous study from Shu et al. (2017) found that dry deposition could cause substantial differences in secondary organic aerosol (SOA) concentrations between two regional chemical transport models (CTMs), the Community Multiscale Air Quality (CMAQ) model, and the Comprehensive Air Quality Model with extensions (CAMx), when accounting for differences in emissions, meteorology, and chemistry. However, a general lack of dry deposition measurements makes it hard to evaluate the accuracy of the model concerning this specific process.

Particle dry deposition is a complex process that depends on the chemical and physical properties of particles, which are related to their source and composition, as well as the features of the underlying land surface and the proximate meteorological conditions. In general, the flux of particle mass through the surface boundary layer is usually mathematically expressed as (Wesely and Hicks, 1977)

$$F(z) = C(z) * V_d, \tag{1}$$

where $F(z)$ is the vertical flux of a pollutant in the surface boundary layer; $C(z)$ is the concentration at a specific height; V_d is the deposition velocity.

In atmospheric models, many mechanistic or process-based dry deposition schemes have been developed to estimate V_d for scientific research and operational purposes (Petroff et al., 2008; Ruijrok et al., 1995) but only a few of them have been implemented in CTMs. Changes to the functional form of the parameterizations are challenges that could cause a variance of estimated V_d by 2 to 3 orders of magnitude (Ruijrok et al. 1995). Land-use dependence is another challenge to either measurement or modeling studies. Zhang (2001) investigated several schemes for calculating particle dry deposition velocity as a function of particle and summarized that some schemes applied only to one type of land-use category (Slinn and Slinn, 1980; Davidson et al., 1982; Wiman and Ågren, 1985; Peters and Eiden, 1992) while others applied to any type of land-use category (Schemel and Hodgson, 1980; Haynie, 1986; Giorgi, 1988). The differences in these studies suggest the importance of using measurements to assess and improve these mechanistic and process-based dry deposition schemes over different land-use categories. However, existing measurements are limited to a few specific land-surface categories (Nemitz et al., 2002). A newly revised particle dry deposition scheme by Emerson et al. (2020) could describe observations across a variety of land-use types, suggesting that they have resolved the deficiencies in dry deposition schemes as a result of the lack of many land-use datasets. However, they also pointed out the difficulty in adapting to a sophisticated scheme in CTMs. As mentioned above, these considerable uncertainties and differences among mechanistic dry deposition schemes make it difficult to select a "best-performing" scheme for use in CTMs. When higher-accuracy mechanistic dry deposition schemes have been chosen, regional models have incorporated physicochemical properties of particles using a variety of approaches, including representing particle modes with a median particle size and standard deviation (e.g., CMAQ, Binkowski and Shankar (1995)), representing the bulk particle population with a single particle diameter (e.g., CAMx coarse-fine approach), or applying the diameter of discrete size bins (e.g., GEOS-Chem Two-Moment Aerosol Sectional model, Emerson et al. (2020)). Saylor et al. (2019) found that fine-particle concentration predictions at the surface may vary by 5%-15% depending on the choice of particle deposition velocity schemes in CTMs. An additional challenge in model evaluation is that most measurement studies report deposition flux for one particle size, making it challenging to assess deposition velocity calculated by regional models directly with measured values. Therefore, it is necessary to translate results among measurements, dry deposition schemes, and regional air quality models to improve large-scale 3-D models' capability to better predict ambient concentrations. Previous reviews (Pryor et al., 2008 and Petroff et al., 2008) have pointed out the value in unified studies that combine numerous measurements and modeling methods.

To further address this gap between measurements and large-scale models, the present study develops a 0-D box model (DepoBoxToolv1.0) to assess dry deposition schemes that have previously been incorporated in 3-D CTMs with available measurement datasets similar to the approach of Khan and Perlinger (2017). We propose two revised schemes to improve dry deposition performance in CMAQv5.3 and compare their performance for different land surface categories with that of several existing dry deposition schemes. These proposed schemes are then incorporated into CMAQ to quantify the change of V_d and resulting concentrations of several particle-phase species of interest. CMAQ performance was evaluated based on available observations of ambient particle concentrations from multiple monitoring networks. Combining the 0-D box model and the 3-D CTM not only helps us better constrain particle dry deposition from both detailed deposition measurements and long-term ambient measurements, but also provides an opportunity to identify missing information from both measurements and models that should be prioritized for future research.

2 Methods

2.1 Description of particle dry deposition schemes

In this study, we focus on two conventional dry deposition schemes, Z01 (Zhang et al., 2001) and PR11 (Pleim and Ran, 2011). These two schemes both borrowed the general framework of Slinn's (1982) scheme but introduced various modifications and alternative forms for the surface resistance (Saylor et al. 2019). They have been widely implemented in regional-scale 3-D models because of their relatively simple formulations and few dependencies on environmental parameters. However, significant deposition differences have been reported by Shu et al. (2017) between CAMx v5.4.1 (Z01) and CMAQ v5.0.1 (PR11). The underlying theory of the two schemes is described in Sections 2.1.1 and 2.1.2. Two revised dry deposition schemes based on the original PR11 are then described in Section 2.1.3.

2.1.1 Z01 scheme

The Z01 scheme, used in CAMx for particle dry deposition, is based on Slinn's (1982) scheme, which was developed for vegetated canopies, including the deposition processes of Brownian diffusion, impaction, interception, gravitational settling and particle rebound. Because the full scheme requires detailed canopy information that is generally unavailable in regional-scale transport models, the underlying formulations were simplified into empirical parameterizations for all deposition processes. In the Z01 scheme, V_d is expressed as

$$V_d = V_g + \frac{1}{R_a + R_s}, \quad (2)$$

where V_g is the gravitational settling velocity; R_a is the aerodynamic resistance above the canopy; R_s is the surface resistance. The gravitational settling velocity is calculated as

$$V_g = \frac{\rho d_p^2 g C}{18\eta}, \tag{3}$$

where ρ is the density of the particle; d_p is the particle diameter; g is the acceleration of gravity; C is the Cunningham correction factor; η is the temperature-dependent viscosity coefficient of air. The Cunningham correction factor C is calculated as

$$C = 1 + \frac{2\lambda}{d_p}\left(1.257 + 0.4e^{-\frac{0.55d_p}{\lambda}}\right), \tag{4}$$

where λ is the mean free path of air molecules and is calculated as the function of temperature, pressure, and the kinematic viscosity of air. The aerodynamic resistance (R_a) is calculated as

$$R_a = \frac{\ln\left(\frac{Z_R}{Z_0}\right) - \Psi_H}{\kappa u_*}, \tag{5}$$

where Z_R is the height at which the dry deposition velocity V_d is evaluated; Z_0 is the roughness length; Ψ_H is the stability function for heat; κ is the Von Karman constant and u_* is the friction velocity. A detailed expression for Ψ_H can be found in Khan and Perlinger (2017).

The surface resistance, R_s depends on the collection efficiency of the surface and is determined by the various deposition processes, the size of the particles, atmospheric conditions, and land surface properties. R_s is usually the limiting resistance for aerosols because Brownian diffusion is much slower for particles than molecular diffusion for gaseous species. However, the effects of inertial impaction and interception by protruding micro-scale roughness elements can partially bridge the diffusion layer such that R_s is inversely related to three collection efficiencies (Slinn, 1982). Brownian diffusion dominates V_d for the smaller particles and declines rapidly with increasing d_p, while impaction and interception are essential for large d_p (e.g., larger than one μm).

In the Z01 scheme, R_s is parameterized as

$$R_s = \frac{1}{\varepsilon_0 u_* (E_B + E_{IM} + E_{IN}) R_1}, \tag{6}$$

where E_B, E_{IM}, E_{IN} are the collection efficiencies from Brownian diffusion, impaction, and interception, respectively; ε_0 is an empirical constant and is taken as 3 for all land-use categories (LUCs). R_1 is the correction factor representing the fraction of particles that stick to the surface and is parameterized as a function of Stokes number (St) as

$$R_1 = e^{-St^{0.5}}, \tag{7}$$

For Brownian diffusion, E_B is parameterized as a function of Schmidt number (Sc),

$$E_B = Sc^{-\gamma}, \tag{8}$$

$$Sc = \frac{\nu}{D}, \tag{9}$$

where Sc is the ratio of kinematic viscosity of air, ν, to the particle Brownian diffusivity (D); γ is a LUC-dependent variable (rough surfaces: 0.54-0.56; smooth surfaces: 0.50-0.56). Brownian diffusivity (D) is calculated as

$$D = \frac{C k_B T}{3\pi\mu d_p}, \tag{10}$$

where C is the Cunningham correction factor; k_B is Boltzmann's constant; and T is temperature.

Particle impaction (E_{IM}) is parameterized as a function of the Stokes number (St), which is the ratio of the stopping distance of a particle to the characteristic dimension of an obstacle (Pryor et al., 2008). One oft-used formulation for St in impaction factor parameterizations tends to emphasize the nature of the flow field in determining the magnitude of St (Giorgi, 1988) and is usually used for smooth surfaces:

$$St = \frac{V_g u_\star^2}{g\nu}, \tag{11}$$

while the formulation of Slinn (1982) focuses on the individual obstacles (e.g., leaves) and is used for vegetation surface:

$$St = \frac{V_g u_\star}{gA}, \tag{12}$$

where A is the characteristic radius of collectors. The assumption for this approach is that vegetative hairs and cobwebs, for example, probably deflect with wind fluctuations, reducing the efficiency with which particles impact on these small collectors. Particle impaction in the Z01 scheme is expressed as

$$E_{IM} = \left(\frac{St}{\alpha + \mathrm{St}}\right)^{\beta}, \tag{13}$$

where α and β are constants. This form is the same as the one used by Peters and Eiden (1992) but α is LUC-dependent and β is assumed to be 2. Collection efficiency by interception (E_{IN}) is calculated as

$$E_{IN} = \frac{1}{2}\left(\frac{d_p}{A}\right)^2, \tag{14}$$

The Z01 scheme is applied in 3-D models (e.g., CAMx and GEOS-Chem) using a single diameter to represent either a discrete size bin (for the sectional aerosol scheme) or bulk aerosol (for the coarse-fine scheme).

2.1.2 PR11 scheme (Pleim and Ran, 2011)

Pleim and Ran (2011) described the equations and techniques used for the particle dry deposition scheme in the CMAQ model (version 4.5 to 5.2.1). V_d is derived by Venkatram and Pleim (1999) and expressed as

$$V_d = \frac{V_g}{1 - e^{-V_g * (R_a + R_b)}}, \tag{15}$$

where V_g has the same formulation as the Z01 scheme and, when calculated using Eq. 3, R_a uses the same expression as Z01, but applies a factor of 0.95 for the Prandtl number under neutral conditions as follows:

$$R_a = 0.95\frac{\ln\left(\frac{Z_R}{Z_0}\right) - \Psi_H}{\kappa u_\star}, \tag{16}$$

R_b is the quasi-laminar boundary layer resistance and expressed as

$$R_b = \left[F_f u_\star (E_B + E_{IM} + E_{IN})\right]^{-1}, \tag{17}$$

where F_f is an empirical correction factor to account for increased deposition in convective conditions as suggested by Binkowski and Shankar (1995):

$$F_f = 1 + 0.24\frac{w_\star^2}{u_\star^2}, \tag{18}$$

where $w_\star$ is the convective velocity scale.

E_B is a function of the Schmidt number and expressed as

$$E_B = Sc^{-\frac{2}{3}}, \tag{19}$$

The Schmidt number was calculated with Eq. 9 identically to the Z01 scheme. Pleim and Ran (2011) expressed E_{IM} as

$$E_{IM} = \left(\frac{St^2}{400+St^2}\right), \tag{20}$$

where Stokes number was calculated with Eq. 11. The value of 400 was chosen for the denominator of the impaction factor calculation to better represent aerosol deposition to heavily vegetated regions. Unlike the CAMx model, the interception efficiency, E_{IN}, is not used in the CMAQ model because it is difficult to specify realistic estimates of these parameters over the area of typical grid cells used by air quality models (i.e., ~4-20km) based on available land-use data (Pleim and Ran, 2011).

The PR11 scheme was applied in CMAQ by integrating the size-dependent terms across each particle mode using the geometric mean diameter and standard deviation (Binkowski and Shankar, 1996). For example, the impaction factor for particle volume was modified to be:

$$\widehat{E_{IM}} = \frac{St^2}{400}\{\exp(20\, ln^2\, \sigma_g)\}, \tag{21}$$

where σ_g is the standard deviation of an aerosol mode. The denominator was simplified from its form in Eq. 20 in order to facilitate incorporation of the integrated Stokes number (Eq. 11). The integrated settling velocity, $\widehat{V_g}$, and integrated Brownian diffusivity, $\widehat{D}$, needed for the Schmidt number, are defined in Appendix A. This form of the impaction term (Eq. 21) is then applied to calculate the boundary-layer resistance (Eq. 17) in the chemical transport model.

2.1.3 Proposed schemes

Although Z01 and PR11 both used Slinn's (1982) scheme as the start point, they also did several modifications, especially for surface resistance, which could be the one of the keys to cause differences. Beyond that, they used different approaches to integrate V_d over particle size distributions after implementing them into regional models (CMAQ: modal approach; CAMx: sectional approach). These differences have been characterized in (Shu et al., 2017), showing that CMAQ (v5.0.1) predicts larger V_d than CAMx (v5.4.1) for large particles. However, these uncertainties have not been constrained in previous studies. In this study, we propose two revised dry deposition schemes that significantly impact the CMAQ-predicted deposition velocities. The two schemes are still based on the existing PR11 scheme with several modifications and better representation of integrations. The first revised scheme (OFF) is set to minimize the influence of σ_g on the integration of impaction. As mentioned in Section 2.1.3, unlike $\widehat{V_g}$ and $\widehat{D}$, the integration form of $\widehat{E_{IM}}$ in Eq. 21 is heavily dependent on σ_g, which could differ its value by tens of thousands of times as the change of σ_g. Especially when it is reaching up to CMAQ upper bound ($\sigma_g = 2.5$), $\widehat{E_{IM}}$ is dominated by the factor of $\exp(20\, ln^2\, \sigma_g)$ rather than impaction of monodisperse particles as Eq. 20. Thus, OFF correctly implements the impaction term following Eq. 20, thereby removing the explicit integration instead of analytical integration across particle size in the expression for E_{IM}. OFF could maximumly avoid the influence of σ_g dependence, however, it also loses the ability to well-representing the polydispersity of the underlying particle size distribution for impaction after these modifications. Therefore, we also propose another

https://doi.org/10.5194/gmd-2021-129
Preprint. Discussion started: 17 May 2021

Geoscientific Model Development Discussions
Open Access

scheme. For the second proposed scheme (VGLAI), we update the impaction term expression from PR11(Eq. 21) to Eq. 22.

$$\widehat{E_{IM}} = \frac{\widehat{St}^2}{\left(1+\widehat{St}^2\right)}, \tag{22}$$

which reduces the constant in the denominator used to approximate the effect of vegetated surfaces to unity as Eq. 20. Accordingly, we modify the expression of the Stokes number to a form that is more suitable for addressing vegetated surfaces:

$$\widehat{St} = \frac{\widehat{V_g} u_\star}{gA}, \tag{23}$$

We integrate the Stokes number by using $\widehat{V_g}$ instead of directly turning off redundant integration factor across particle size for each aerosol mode like OFF, thus the polydispersity of the underlying particle size distribution is implicitly accounted for. Finally, we add a new leaf area index (LAI) factor in R_b to respond to vegetation coverage by representing the greater surface area of leaves,

$$R_b = \left[\left(1 + f_{veg}(LAI - 1)\right) \cdot F_f u_\star (E_B + E_{IM} + E_{IN})\right]^{-1}, \tag{24}$$

where f_{veg} is the fractional area of vegetation surface in the CMAQ grid cell, which can be acquired from the inputs to typical meteorological models (i.e. the Weather Research and Forecasting model; WRF) and lai is the leaf area index in the vegetated portion. E_B and E_{IN} both inherit implementation in PR11.

2.2 Assessment of particle dry deposition schemes at different model scales

We conducted a comprehensive evaluation of particle dry deposition schemes discussed in Section 2.1 at different model scales. All tested schemes and their full expressions are presented in Table 1. We first developed a convenient and unified 0-D box model (DepoBoxToolv1.0) and evaluated the schemes on three different vegetation surface categories (grass, coniferous forest and deciduous forest). For better understanding the performance of the schemes across atmospherically relevant particle sizes, we investigated the predicted deposition velocities for a variety of modal diameters and standard deviations. In section 2.2.1, we describe the details of DepoBoxToolv1.0, and we present the measurements used for evaluating this box model in section 2.2.2. Finally, in section 2.2.3, we describe how we have incorporated the two newly proposed dry deposition schemes (OFF and VGLAI) in CMAQv5.3 and characterized them alongside the existing scheme (PR11).

2.2.1 Development and application of DepoBoxToolv1.0 platform

DepoBoxToolv1.0 (https://github.com/shumarkq/Depoboxtool/tree/master) is an open-source, Python-based tool that can be easily used, modified, and distributed throughout the research community to help translate between deposition models and measurements. DepoBoxToolv1.0 currently provides four essential functions including dry deposition scheme evaluation, diagnostics, sensitivity analysis, and model inter-comparison. Further, it can easily incorporate different land-use categories when corresponding parameters are available. In this study, we selected three measurement studies prescreened from Khan and Perlinger (2017), and details are described in

Section 2.2.2. In the future, DepoBoxTool may be applied to better understand field measurements of particle deposition above surfaces of varying types.

Fundamentally, DepoBoxToolv1.0 can quickly toggle multiple schemes for inter-comparison while isolating the predictions from the uncertainties from other photochemical modeling processes. This feature is useful for better constraining the uncertainty introduced by the choice of numerical approximation to represent the particle size distribution. DepoBoxToolv1.0 has the option of calculating V_d for a single-diameter particle population, for a number of discrete size bins (i.e. sectional aerosol approach), or for a log-normal mode (i.e. modal aerosol approach); each approach is regularly used in 3-D models. DepoBoxToolv1.0 does not explicitly treat varying chemical composition with size, but this feature may be added if detailed measurements are available in the future.

We applied both the modal and the sectional size distributions in the DepoBoxToolv1.0 to compare with a single diameter approach. Appendix A describes how parameters like settling velocity and Brownian diffusion are extended, with knowledge of d_p and σ, to apply to the modal approach. Size-dependence was thus introduced through these terms and propagated through the calculated of V_d for the OFF and VGLAI schemes. For the PR11 scheme, additional integration was applied for the impaction factor calculation (Eq. 21). Because we are focused primarily in this study on improving the representation of dry deposition in CMAQ, we did not consider the modal integration of the Z01 scheme.

For the application of the sectional approach, we calculated particle numbers at each defined bin between lower and upper particle diameter bounds using Eq. 25

$$N(d_p) = \frac{N_t}{2} + \frac{N_t}{2}\operatorname{erf}\left(\frac{\ln\left(d_p/\overline{d_{pg}}\right)}{\sqrt{2}ln\sigma_g}\right), \quad (25)$$

where N_t is the total number of particles; d_p is the particle diameter; and $\overline{d_{pg}}$ is the median diameter. Number-weighted dry deposition velocity was estimated as the sum of normalized velocities at each size bin using Eq. 26

$$V_d = \sum\left(\frac{N_i}{N_t} * V_{d_i}\right), \quad (26)$$

where N_i is the number of particles at each size bin. For aerosol volume, the initial volume at each bin was calculated first using Eq. 27 and assuming uniform density across particle sizes.

$$M_i = \rho * V_i \ = \rho * \frac{\pi}{6} * d_{pm_i}^3 * N_i, \quad (27)$$

The volume-weighted dry deposition velocity is computed as the sum of normalized velocities at each size bin using Eq. 28

$$V_d = \sum\left(\frac{V_i}{\sum V_i} * V_{d_i}\right), \quad (28)$$

where V_i and M_i are the volume and mass of particles in section i, respectively. The dry deposition velocity (V_{d_i}) is calculated using d_{pm_i}(the mean diameter at each bin). We use 100 size bins for calculations to minimize numerical artifacts (see Supplement).

Finally, we used DepoBoxToolv1.0 to conduct a sensitivity analysis exploring the effects of the underlying particle size distribution (median particle diameter and standard deviation) on the predictions of each experimental scheme (Z01, OFF, and VGLAI) relative to the PR11 scheme. For this exercise, every scheme is applied via the sectional approach. We test a wide range of diameters from 0.01 to 50 μm and standard deviations from 1.01 to 2.5

https://doi.org/10.5194/gmd-2021-129
Preprint. Discussion started: 17 May 2021

for a log-normal particle size distribution and use N_B to characterize the difference among schemes. Results are discussed in Section 3.2.

2.2.2 Field measurements for DepoBoxToolv1.0

Khan and Perlinger (2017) compiled available measured V_d, inferred V_d, and relevant physical and environmental parameters (Table 2). Unfortunately, although these studies provide useful observations, we omitted many of them in our study because they did not provide the required parameters for running DepoBoxToolv1.0. Three measurement studies were chosen to evaluate deposition schemes for three sizes of particles on grass (Vong et al., 2004), coniferous forest (Lamaud et al., 1994), and deciduous forests (Matsuda et al., 2010). These three studies each used different methods to measure aerosol fluxes across particle sizes. Lamaud et al. (1994) and Vong et al. (2004) both used eddy correlation methods and measured aerosol number while Matsuda et al. (2010) used gradient methods and measured aerosol volume. Lamaud et al. (1994) reported the log-normal particle size distribution with 0.04 μm geometric mean diameter (d_{pg}) and 2.5 geometric standard deviation (σ_g) to represent particles on the coniferous forest. Vong et al. (2004) reported deposition velocity for four particle sizes but expressed the most confidence and representativeness in the results for d_{pg} = 0.52 μm. Vong et al. (2004) did not characterize the geometric standard deviation, so we have assumed two values (σ_g= 1.7 and 2.5) that are often associated with the shape of background particle distributions for comparison with the grass dataset. Matsuda et al. (2010) did not provide a detailed size distribution. Thus, 0.48 μm (Kenneth et al., 1977) was assumed to be the d_{pg} of reported sulfate $PM_{2.5}$ particles for the deciduous forest dataset. We also assumed values for σ_g of 1.7 and 2.5 as was done for Vong et al. (2004). Table 2 shows site information and required parameters for running DepoBoxToolv1.0 from the three selected measurement studies. In order to run the PR11 dry deposition scheme in DepoBoxToolv1.0, the convective velocity scale, $w_\star$, was provided by meteorological model (WRF) output since it is absent in the selected measurement studies. An estimation of $w_\star$ involves a knowledge of the surface heat flux and the mixed layer height and it is not practical to measure these variables on a routine basis (Venkatram, 1978). A representative $w_\star$ for a specific season and the land surface condition is assumed to reproduce a similar value of $w_\star$ to the values that would be typical for the field site. Median values of assumed $w_\star$ for the three measurement studies are presented in Table 2 and detailed daily variations of assumed $w_\star$ (Fig. S2) can be found in the supplement.

2.2.3 CMAQ simulation and observational data sets

We conducted three CMAQ simulations including the conventional deposition scheme (PR11), the scheme with improved impaction (OFF) and the scheme with larger sensitivity to vegetation (VGLAI) for July 2011. The modeling domain is a grid with 12 km x 12 km resolution covering the entire conterminous U.S. and extending to 50 hPa in altitude with 35 vertical layers and higher resolution near the Earth's surface. The lowest model layer is approximately 20 meters deep. Emissions for 2011 are tabulated from information provided by states and other federal agencies via the 2011 National Emissions Inventory. The emissions estimates were further allocated in space and time by the Sparse Matrix Operator Kernel Emissions (SMOKE) program. Plume rise for elevated point sources was calculated online in CMAQ, as were NO_x emissions from lightning strikes (Kang et al., 2019). Biogenic emissions of volatile organic compounds were predicted with the Biogenic Emission Inventory System (Bash et al., 2016) and Offline meteorology was calculated with the Weather Research and Forecasting (WRF) model version 3.7. Boundary conditions for the model were driven by a hemispheric application of the GEOS-Chem model (Henderson et al., 2014) run for 2011. Specific land cover information was obtained from the National Land Cover Database (NLCD) and leaf area index information was gathered from satellite products from the MODIS satellite. Outputs from the three CMAQ simulations was paired in space and time with observed data using the atmospheric model evaluation tool (AMET, Appel et al., 2011). There are several regional and national networks that provide routine observations of particle species in the U.S. for CMAQ evaluation. In this study, we used SO4 measurement data sets from the Interagency Monitoring of Protected Visual Environments (IMPROVE, 157 sites; http://vista.cira.colostate.edu/improve/, last access: 21 July 2018) and Chemical Speciation Network (CSN; 171 sites; https://www3.epa.gov/ttnamti1/speciepg.html, last access: 21 July 2018). Appel et al. (2011) showed that a recent version of CMAQ (v5.1) demonstrates impressive model skill predicting ambient fine PM concentrations when compared with routine measurement networks, including CSN and IMPROVE network. Nolte et al. (2015) investigated fine and coarse mode size distribution performance for CMAQv5.0, finding that many sites and chemical species contributions were well-reproduced, but the model tended to underpredict concentrations of large particles in sites dominated by soil dust. Appel et al. (2020) compared metrics (concentration, bias, root mean square error (RMSE) and the Pearson correlation coefficient (COR)) of monthly average $PM_{2.5}$ between CMAQv5.2.1 (PR11) and CMAQv5.3.1 (VGLAI) and found that results of CMAQv.5.3.1 are expectedly better than CMAQv5.2.1.

2.2.4 Evaluation metrics

Two statistical metrics are used in this study. Fractional Bias (F_B) is used to evaluate our model results and is calculated as

$$F_B = \frac{2}{N}\sum\frac{M_i - O_i}{M_i + O_i}, \tag{29}$$

N is the number of data points; M_i is modeled concentration or V_d; O_i is observed concentration or V_d. In DepoBoxToolv1.0, we use F_B to evaluate the dry deposition schemes with site observations. F_B is also used to evaluate CMAQ performance with observations collected from routine measurement networks (Section 3.5).

Normalized bias (N_B) is used for quantifying the change in predictions from the PR11 base deposition scheme to one of the other schemes (Z01, OFF or VGLAI) for both the size distribution sensitivity analysis with DepoBoxToolv1.0 and the full 3D CMAQ simulations. It is calculated as

$$N_B = \frac{M_{m_i} - M_{b_i}}{M_{b_i}}, \tag{30}$$

where M represents any metric (i.e., V_d or pollutant concentrations); b_i is the result of PR11 dry deposition scheme; m_i is the result of one of the other dry deposition schemes.

https://doi.org/10.5194/gmd-2021-129
Preprint. Discussion started: 17 May 2021

Geoscientific Model Development Discussions
Open Access EGU

3 Results

3.1 Evaluation of dry deposition schemes in DepoBoxToolv1.0

We predict V_d with four deposition schemes (Z01, PR11, OFF, VGLAI) by using measured parameters and meteorological data from ambient field studies as box model inputs, except $w_\star$ which comes from WRF. Daily variations of measured and modeled V_d for three land-use categories (grass, coniferous and deciduous forests) calculated using sectional and modal approaches are presented in Fig. 1-3, respectively. Single diameter results are shown in Fig. S4. We found that Z01 (CAMx) performed very differently versus the other three PR11-based schemes for the three different land-use types (Table 3). For the grass dataset, all schemes markedly underestimate the measured V_d with low fractional biases down to -1.40 (Fig. 1). Over the coniferous forest, Z01 and VGLAI overestimate the measured V_d while PR11 and OFF underestimate the measured V_d (Fig. 2). For grass and coniferous forest comparisons where aerosol numbers are reported (k=0), the predictions do not appear highly sensitive to the choice of size distribution method. Although we reproduced the same deposition velocities with the measurement data as in Vong et al. (2004) for grass, our box model is unable to reproduce the same bimodal pattern for all four deposition schemes. This could be explained by the imperfection of observation data since the measurement could not be perfectly considered to represent "deposition to the grass surfaces" because they have not been screened for either wind direction or the morning transition period (Vong et al., 2004). For the deciduous forest where aerosol volumes are used (k=3), estimated V_d is very sensitive to σ_g. When changing σ_g from 1.7 to 2.5, all schemes using either sectional or modal methods sharply increase V_d from underestimating (FB < -1.52) to overestimating (FB > 0.69; Table 3 and Fig. 3). The PR11 scheme particularly stands out, overpredicting V_d by an order of magnitude relative to measured V_d when σ_g = 2.5. Considering the lack of information that we had about the shape of the size distributions when the measurements were made, we cannot constrain the modeled V_d merely based on box model results. However, with the same σ_g (2.5), the updated schemes (OFF and VGLAI) both reduce the bias in V_d compared to PR11. This suggests that the overestimated V_d in the PR11 scheme could be caused by the modal size integration of the impaction term (Eq. 21). Both OFF and VGLAI resolve this potential error by turning off impaction integration and relying on the integrated settling velocity to calculate Stokes number. Across three land-use types, PR11, OFF, and VGLAI show more consistent diurnal patterns as the measurements than Z01, indicating that convective velocity scale, $w_\star$ (Fig. S2) could drive the diurnal pattern. Beyond that, all schemes' results are very sensitive to σ_g, especially when aerosol volumes are used in Matsuda et al. (2010), suggesting the importance of the measured σ_g when assessing modeled V_d.

3.2 Sensitivity of deposition schemes to particle size distribution

The range of behaviors for each dry deposition scheme were explored using DepoBoxToolv1.0 to calculate the aggregate deposition velocity (using a 100 size bin sectional approach) of a population of particles for a wide range of atmospherically relevant d_{pg} (0.01~50 μm) and σ_g (1.01~2.5). From the left column of Fig. 4, we can see that, in general, V_d by Z01 are lower than PR11 for grass and deciduous forest, with some exceptions at tiny sizes (d_p < 0.1 μm) over deciduous forest. For coniferous forest, Z01 has higher V_d for small particles ($d_p <$ 1.0 μm) and

https://doi.org/10.5194/gmd-2021-129
Preprint. Discussion started: 17 May 2021

Geoscientific Model Development Discussions

lower V_d when d_p is larger than 1.5 μm. As shown in the middle column of Fig. 4, OFF generally predicts lower V_d for groups of particles where d_p is from 0.5 to 10 μm and σ_g is from 1.2 to 2.5 on all three surface categories. For these regimes, impaction dominates the change of V_d. Deviations relax though at the smallest and largest particle sizes, depending on the standard deviation of the aerosol mode. In the right column of Fig. 4, VGLAI has a similar V_d as OFF across particle mean diameters and mode widths for grass but predicts sharp increases in V_d for small particles ($d_p < 1.5$ μm) and decreases for large particles ($d_p > 1.5$ μm) on both coniferous and deciduous forests. This divergent tendency of V_d with the change of d_p can be explained by two competing factors in VGLAI. When particles are small, impaction will not dominate V_d, and the new vegetation dependence will increase V_d. When particles are large, impaction dominates V_d, and the vegetation factor cannot offset the decrease of V_d due to updating impaction with the revised integration technique. Thus, at large particle sizes as well as under lower LAI condition such as grass, the deviations of OFF and VGLAI relative to PR11 look more similar.

3.3 Comparison of dry deposition schemes in CMAQ

The DepoBoxToolv1.0 analysis gives some indication of the potential impact of revising the PR11 scheme that is used in CMAQv5.2.1 and earlier with one of the two proposed schemes. However, these box model results are limited to three land-use surface categories and may not reflect performance in CMAQ for broader conditions and multiple land-use surfaces. To characterize the impact of the OFF and VGLAI schemes in CMAQ, we cluster the dry deposition velocities and fluxes of some species of interest across the entire domain into two categories. Spatially averaged particle dry deposition velocities above forest and non-forested areas are compared between three schemes for fine, accumulation, and coarse mode particles in CMAQ. From the spatiotemporal averages shown in Fig. 5A, OFF and VGLAI both reduce V_d by approximately 1060% and 340% compared to the PR11 simulation for coarse-mode particles (d_p > 0.2 μm). For Aitken-mode particles (d_p <0.1 μm), OFF does not change V_d while VGLAI increases V_d by ~300%. For accumulation mode particles (0.08 μm < d_p < 0.2 μm), VGLAI has a similar V_d as PR11 while OFF reduces V_d by ~250%. Figure 5B shows that modeled V_d on the non-forested surface presents a similar pattern as on the forest surface but has systematically lower modeled V_d (note the y-axis difference). Figure 6 illustrates the impact of the revised deposition schemes on spatially averaged concentrations of fine-mode SO_4 (ASO4I+J), and speciated coarse-mode components including coarse-mode SO_4 (ASO4K), coarse-mode soil species (ASOIL), coarse-mode primary anthropogenic mass (ACORS), and coarse-mode sea-spray cations (ASEACAT) above the forest and non-forested surfaces. From Fig. 6, OFF increases fine and coarse SO_4 particle concentrations slightly over both forest and non-forested surfaces. VGLAI reduces fine SO_4 particle concentrations slightly but not much change from the PR11 case is observed at this domain-wide scale. Results for ASOIL, ACORS and ASEACAT demonstrate that both the OFF and VGLAI schemes increase wind-blown dust (forest/non-forested: OFF=255%/127%, VGLAI=120%/81%), anthropogenic dust (213%/82%, 132%/59%) and sea-spray aerosol (186%/61%, 110%/52%) mass concentration predictions significantly in most cases. However, the change of concentrations due to changing dry deposition varies among species based on the spatial distribution of their emissions and the likelihood of each type being transported over relevant land-use types.

https://doi.org/10.5194/gmd-2021-129
Preprint. Discussion started: 17 May 2021

3.4 Spatial particle dry deposition velocity differences in CMAQ

Figure 7 spatially compares dry deposition velocities of three sizes of SO_4 particles (Aitken, accumulation, coarse)) for the three schemes (PR11, OFF, VGLAI) implemented in CMAQ. There generally exists orders of magnitude difference in V_d among different sizes of SO_4 particles (Aitken: V_d = 0.03~0.4 cm/s, accumulation: V_d = 0.02~0.1 cm/s, coarse: V_d = 0.4~10 cm/s). On a nationwide scale, V_d can be very different as a result of mixed land-use categories. In Fig. 7, we see V_d in the mid-east U.S. is systematically lower than in other U.S. regions for all three sizes of SO_4 particles, following the distribution of eastern deciduous forests (Dyer, 2006). The three CMAQ simulations have significant differences in V_d across the U.S. Compared with the PR11 model, OFF systematically reduces the V_d of coarse SO_4 particles by 96%. For smaller particles, OFF has less impact than on large particles but still reduces V_d by up to 35% for the Aitken mode and 96% for the accumulation mode. By removing the explicit integration of the impaction term we discussed in Section 2.2.2 (i.e. moving PR11 to OFF), we systematically reduce V_d for all sizes of particles. VGLAI predicts similar V_d for coarse particles like OFF but systematically increases V_d by 7.8%~319% for the Aitken mode. For accumulation mode particles, VGLAI shows spatial diversity of V_d and even increases V_d in some regions, which indicates that we could offset changes from the impaction factor revision with other uncertainties from a more detailed vegetation dependence.

3.5 Spatial SO_4 particle concentration differences in CMAQ

Small differences in spatially averaged SO_4 particle concentrations shown in Fig. 6 suggest that further temporal and spatial characterization of the dry deposition influence on concentration is needed because dry deposition velocities and fluxes also vary temporally and spatially. Figure 8 shows the spatial SO_4 concentration differences between the three CMAQ simulations. We examined both coarse (ASO4K) and fine (ASO4IJ) mode SO_4 concentrations but only evaluated modeled fine concentrations using available measured data at the IMPROVE and CSN monitoring sites. As shown in Fig. 8A-F, OFF and VGLAI both have a more significant influence on coarse SO_4 than on fine SO_4 concentrations. The OFF case systematically increases SO_4 concentrations (coarse: Percent change = 3%-395%; fine: PC= 0.1%-21%). VGLAI shows a spatial pattern of SO_4 concentration that changes with land-use (coarse: PC = -76% to +336%; fine: PC = -7% to +18%). The vegetation factor increases V_d in vegetation areas by providing more surface area for deposition. The vegetation fraction specified the Pleim-Xiu land-surface model (PX LSM, Xiu and Pleim, 2001) used in WRFv3.7 was overestimated, leading to a smaller R_b (Eq. 24). We expect very different results when using newer versions of WRF (v4.0 or later) when the vegetation fractions used in the PX LSM were substantially reduced (more realistic), especially in much of the western US. The fractional bias in predicted fine SO_4 concentrations versus air quality measurement network sites for PR11 and the relative change of F_B between OFF and VGLAI relative to PR11 are presented in Fig. 9A-C. In Fig. 9A, we can see that there is a systematic low bias at IMPROVE and CSN sites for fine sulfate. In Fig. 9B, OFF reduces the low-bias for all sites in the entire U.S., by as much as 21% for the sites in the mid-east U.S. In Fig. 9C, VGLAI reduces low-bias by as much as 1% for selected sites in the mid-east U.S. but conversely increases the low-bias by up to 13% for selected sites in the rest of U.S where non-forested surface dominates.

4 Conclusions

This study investigated particle dry deposition by characterizing critical parameters and land-use dependence in a box model and in a regional-scale 3-D chemical transport model. A land-use dependent deposition scheme box model was developed to evaluate and diagnose particle dry deposition algorithms. Although the accuracy of each mechanistic dry deposition scheme varied considerably with land-use type, the results show that the scheme by Pleim and Ran (2011) modified to include vegetation dependence was best able to capture the magnitude and variability across all of the observation datasets.

The influence of mechanistic dry deposition schemes on regional model predictions can be difficult to disentangle from uncertainties introduced by the choice of numerical approach used to simulate the size distribution, representation of other source and sink processes, spatiotemporal variation in environmental inputs (e.g. vegetation fraction and LAI), and sub-grid variability in land-use type. For example, differences in calculating dry deposition velocity between sectional and modal methods can lead to discrepancies as large as a factor of 4 for particle sizes of 0.5 μm over deciduous forests. Rather than investigate the performance of the dry deposition scheme in a large, operational domain, we performed evaluation by land-use type.

Combining the results of the DepoBoxToolv1.0 and CMAQ analyses, we think the VGLAI scheme is most applicable for predicting particle dry deposition over grass and coniferous forests in CMAQ. For deciduous forests, it is difficult to constrain the deposition schemes with observations since particle diameter and standard deviation for sulfate $PM_{2.5}$ particles are assumed in this study. A better understanding of the impact of the particle size distributions as well as other forest processes important for deposition will be helpful for further constraining large-scale model predictions. For example, particle deposition velocity predictions were quite sensitive to the standard deviation of the size distribution, especially for larger particles where the deposition velocity changes by orders of magnitude with relatively small changes in particle size. We noted that the base PR11 strongly overpredicted V_d for large particles (1~10 μm) compared to OFF and VGLAI schemes, suggesting that an artificial bias introduced from integrating the impaction factor has been alleviated. The corresponding impact of updating from PR11 to VGLAI in CMAQ is more significant for coarse-mode particles than accumulation mode. CMAQ simulations OFF and VGLAI show that for fine particles, OFF has slower spatially averaged V_d than PR11 while VGLAI has faster V_d than PR11. In VGLAI, the vegetation factor increased V_d on vegetation areas by providing more turbulent surface resistance when impaction does not dominate V_d for small particles.

We have bridged the gap between dry deposition measurement and modeling by rigorous use of box model frameworks, regional transport model platforms and field measurements but more efforts are needed for better understanding particle dry deposition. This study highlighted that deviation among deposition schemes is most pronounced for small and large particles while current measurements focus on accumulation-mode relevant diameters. To constrain this uncertainty, more observations on small (d_p < 50 nm) and large (d_p > 2.5 μm) particles are needed for evaluation. By building the bridge to understand particle dry deposition from in situ measurements to a simple simulated atmospheric modeling system, this study better links CMAQ predictions to available real-world observations and incrementally reduces uncertainties in the magnitude of loss processes important for the lifecycle of atmospheric pollutants relevant for human and ecosystem exposure.

https://doi.org/10.5194/gmd-2021-129
Preprint. Discussion started: 17 May 2021

Geoscientific Model Development Discussions

Appendix A. Integration of dry deposition schemes for modal aerosol models

Current air quality models compute V_d as a function of particle diameter. Two typical methods to represent aerosol size distributions are with discrete size bins or with log-normal modes (Riemer et al., 2019). The CMAQ aerosol module uses a trimodal log-normal distribution to represent particles in the sub-micrometer size range. As a result, polydisperse properties are calculated as functions of the modal-based parameters. The polydisperse formulation for aerosol diffusivity may be written as

$$\widehat{D} = D\left\{\exp\left(\frac{-2k+1}{2} ln^2 \sigma_g\right) + 1.246Kn_g \exp\left(\frac{-4k+4}{2}\right) \ln^2 \sigma_g\right\}. \quad (A1)$$

while the polydisperse settling velocity may be written as

$$\widehat{V_g} = V_g\left\{\exp\left(\frac{4k+4}{2} ln^2 \sigma_g\right) + 1.246Kn_g \exp\left(\frac{2k+1}{2}\right) \ln^2 \sigma_g\right\}. \quad (A2)$$

where k is equal to the index of the moment being integrated, $Kn_g = \frac{2\lambda}{d_p}$; σ_g is the geometric standard deviation of log-normal size distribution. D and V_g are first calculated using Eqs. 10 and 3 with the geometric mean diameter (d_{pg}) and then integrated over each mode using Eqs. A1 and A2, respectively. CMAQ calculates particle dry deposition velocity based on aerosol number, surface area and volume using Eqs. A3-A5. For aerosol number (k = 0),

$$\widehat{E_{IM}} = E_{IM}\{\exp(8\, ln^2 \sigma_g)\}. \quad (A3)$$

For aerosol surface area (k = 2),

$$\widehat{E_{IM}} = E_{IM}\{\exp(16\, ln^2 \sigma_g)\}. \quad (A4)$$

For aerosol volume (k = 3),

$$\widehat{E_{IM}} = E_{IM}\{\exp(20\, ln^2 \sigma_g)\}. \quad (A5)$$

Code and Data availability

Depoboxtoolv1.0 source code is freely available from http://doi.org/10.5281/zenodo.4749636 (Shu et al., 2021) under the Creative Commons Attribution 4.0 International. It also includes the code and data for testing all box model results in this study. CMAQ source code, including updated particle dry deposition scheme (VGLAI), is freely available via http://github.com/usepa/cmaq.git. Archived CMAQ versions including previous particle dry deposition scheme (PR11) are available from the same repository. The code and data for CMAQ analysis results are also available from http://doi.org/10.5281/zenodo.4749758 (Shu et al., 2021) under the Creative Commons Attribution 4.0 International.

Supplement

The supplement related to this article is available online.

Author contributions

QS and BM designed the research scope. QS and JEP built the model code. BM and KWA performed the simulations. All authors participated in data curation and/or analysis. QS led the development of this manuscript and drafted the initial manuscript. QS, BM, and BHH were responsible for most of the draft revisions, and all authors contributed to the subsequent drafts.

Competing interests

The authors declare that they have no conflict of interests.

Disclaimer

The views expressed in this article are those of the authors and do not necessarily represent the views or policies of the U.S. Environmental Protection Agency.

Acknowledgments

This project was supported in part by an appointment to the Research Participation Program at the Office of Research and Development, US Environmental Protection Agency, administered by the Oak Ridge Institute for Science and Education through an interagency agreement between the US Department of Energy and the EPA.

References

Appel, K. W., Gilliam, R. C., Davis, N., Zubrow, A., and Howard, S. C.: Overview of the atmospheric model evaluation tool (AMET) v1.1 for evaluating meteorological and air quality models, Environ. Model. Softw., 26, 434–443, https://doi.org/10.1016/j.envsoft.2010.09.007, 2011.

Appel, K. W., Bash, J. O., Fahey, K. M., Foley, K. M., Gilliam, R. C., Hogrefe, C., Hutzell, W. T., Kang, D., Mathur, R., Murphy, B. N., Napelenok, S. L., Nolte, C. G., Pleim, J. E., Pouliot, G. A., Pye, H. O. T., Ran, L., Roselle, S. J., Sarwar, G., Schwede, D. B., Sidi, F. I., Spero, T. L., and Wong, D. C.: The Community Multiscale Air Quality (CMAQ) Model Versions 5.3 and 5.3.1: System Updates and Evaluation, Geosci. Model Dev. Discuss., 1–41, https://doi.org/10.5194/gmd-2020-345, 2020.

Bash, J. O., Baker, K. R., and Beaver, M. R.: Evaluation of improved land use and canopy representation in BEIS v3.61 with biogenic VOC measurements in California, Geosci. Model Dev., 9, 2191–2207, https://doi.org/10.5194/gmd-9-2191-2016, 2016.

Binkowski, F. S. and Shankar, U.: The Regional Particulate Matter Model: 1. Model description and preliminary results, J. Geophys. Res. Atmospheres, 100, 26191–26209, https://doi.org/10.1029/95JD02093, 1995.

Davidson, C. I., Miller, J. M., and Pleskow, M. A.: The influence of surface structure on predicted particle dry deposition to natural grass canopies, Water. Air. Soil Pollut., 18, 25–43, https://doi.org/10.1007/BF02419401, 1982.

Dyer, J. M.: Revisiting the Deciduous Forests of Eastern North America, BioScience, 56, 341–352, https://doi.org/10.1641/0006-3568(2006)56[341:RTDFOE]2.0.CO;2, 2006.

https://doi.org/10.5194/gmd-2021-129
Preprint. Discussion started: 17 May 2021

Emerson, E. W., Hodshire, A. L., DeBolt, H. M., Bilsback, K. R., Pierce, J. R., McMeeking, G. R., and Farmer, D. K.: Revisiting particle dry deposition and its role in radiative effect estimates, Proc. Natl. Acad. Sci., 117, 26076–26082, https://doi.org/10.1073/pnas.2014761117, 2020.

Giorgi, F.: Dry deposition velocities of atmospheric aerosols as inferred by applying a particle dry deposition parameterization to a general circulation model, Tellus B Chem. Phys. Meteorol., 40, 23–41, https://doi.org/10.3402/tellusb.v40i1.15627, 1988.

Henderson, B. H., Akhtar, F., Pye, H. O. T., Napelenok, S. L., and Hutzell, W. T.: A database and tool for boundary conditions for regional air quality modeling: description and evaluation, Geosci. Model Dev., 7, 339–360, https://doi.org/10.5194/gmd-7-339-2014, 2014.

Kang, D., Pickering, K. E., Allen, D. J., Foley, K. M., Wong, D. C., Mathur, R., and Roselle, S. J.: Simulating lightning NO production in CMAQv5.2: evolution of scientific updates, Geosci. Model Dev., 12, 3071–3083, https://doi.org/10.5194/gmd-12-3071-2019, 2019.

Khan, T. R. and Perlinger, J. A.: Evaluation of five dry particle deposition parameterizations for incorporation into atmospheric transport models, Geosci. Model Dev., 10, 3861–3888, https://doi.org/10.5194/gmd-10-3861-2017, 2017.

Lamaud, E., Brunet, Y., Labatut, A., Lopez, A., Fontan, J., and Druilhet, A.: The Landes experiment: Biosphere-atmosphere exchanges of ozone and aerosol particles above a pine forest, J. Geophys. Res. Atmospheres, 99, 16511–16521, https://doi.org/10.1029/94JD00668, 1994.

Lovett, G. M.: Atmospheric Deposition of Nutrients and Pollutants in North America: An Ecological Perspective, Ecol. Appl., 4, 629–650, https://doi.org/10.2307/1941997, 1994.

Matsuda, K., Fujimura, Y., Hayashi, K., Takahashi, A., and Nakaya, K.: Deposition velocity of PM2.5 sulfate in the summer above a deciduous forest in central Japan, Atmos. Environ., 44, 4582–4587, https://doi.org/10.1016/j.atmosenv.2010.08.015, 2010.

Nemitz, E., Gallagher, M. W., Duyzer, J. H., and Fowler, D.: Micrometeorological measurements of particle deposition velocities to moorland vegetation, Q. J. R. Meteorol. Soc., 128, 2281–2300, https://doi.org/10.1256/qj.01.71, n.d.

Nolte, C. G., Appel, K. W., Kelly, J. T., Bhave, P. V., Fahey, K. M., Collett Jr., J. L., Zhang, L., and Young, J. O.: Evaluation of the Community Multiscale Air Quality (CMAQ) model v5.0 against size-resolved measurements of inorganic particle composition across sites in North America, Geosci. Model Dev., 8, 2877–2892, https://doi.org/10.5194/gmd-8-2877-2015, 2015.

Peters, K. and Eiden, R.: Modelling the dry deposition velocity of aerosol particles to a spruce forest, Atmospheric Environ. Part Gen. Top., 26, 2555–2564, https://doi.org/10.1016/0960-1686(92)90108-W, 1992.

Petroff, A., Mailliat, A., Amielh, M., and Anselmet, F.: Aerosol dry deposition on vegetative canopies. Part I: Review of present knowledge, Atmos. Environ., 42, 3625–3653, https://doi.org/10.1016/j.atmosenv.2007.09.043, 2008.

Pleim, J. and Ran, L.: Surface Flux Modeling for Air Quality Applications, Atmosphere, 2, 271–302, https://doi.org/10.3390/atmos2030271, 2011.

Pryor, S. C., Gallagher, M., Sievering, H., Larsen, S. E., Barthelmie, R. J., Birsan, F., Nemitz, E., Rinne, J., Kulmala, M., Grönholm, T., Taipale, R., and Vesala, T.: A review of measurement and modelling results of particle atmosphere–surface exchange, Tellus B Chem. Phys. Meteorol., 60, 42–75, https://doi.org/10.1111/j.1600-0889.2007.00298.x, 2008.

Riemer, N., Ault, A. P., West, M., Craig, R. L., and Curtis, J. H.: Aerosol Mixing State: Measurements, Modeling, and Impacts, Rev. Geophys., 57, 187–249, https://doi.org/10.1029/2018RG000615, 2019.

https://doi.org/10.5194/gmd-2021-129
Preprint. Discussion started: 17 May 2021

Geoscientific Model Development
Discussions

Ruijrok, W., Davidson, C. I., and Nicholson, K. W.: Dry deposition of particles, Tellus B, 47, 587–601, https://doi.org/10.1034/j.1600-0889.47.issue5.6.x, 1995.

Saylor, R. D., Baker, B. D., Lee, P., Tong, D., Pan, L., and Hicks, B. B.: The particle dry deposition component of total deposition from air quality models: right, wrong or uncertain?, Tellus B Chem. Phys. Meteorol., 71, 1550324, https://doi.org/10.1080/16000889.2018.1550324, 2019.

Shu, Q., Koo, B., Yarwood, G., and Henderson, B. H.: Strong influence of deposition and vertical mixing on secondary organic aerosol concentrations in CMAQ and CAMx, Atmos. Environ., 171, 317–329, https://doi.org/10.1016/j.atmosenv.2017.10.035, 2017.

Slinn, S. A. and Slinn, W. G. N.: Predictions for particle deposition on natural waters, Atmospheric Environ. 1967, 14, 1013–1016, https://doi.org/10.1016/0004-6981(80)90032-3, 1980.

Slinn, W. G. N.: Precipitation chemistryPredictions for particle deposition to vegetative canopies, Atmospheric Environ. 1967, 16, 1785–1794, https://doi.org/10.1016/0004-6981(82)90271-2, 1982.

Venkatram, A.: Estimating the convective velocity scale for diffusion applications, Bound.-Layer Meteorol., 15, 447–452, https://doi.org/10.1007/BF00120606, 1978.

Venkatram, A. and Pleim, J.: The electrical analogy does not apply to modeling dry deposition of particles, Atmos. Environ., 33, 3075–3076, https://doi.org/10.1016/S1352-2310(99)00094-1, 1999.

Vong, R. J., Vickers, D., and Covert, D. S.: Eddy correlation measurements of aerosol deposition to grass, Tellus B, 56, 105–117, https://doi.org/10.1111/j.1600-0889.2004.00098.x, 2004.

Wesely, M. L. and Hicks, B. B.: Some Factors that Affect the Deposition Rates of Sulfur Dioxide and Similar Gases on Vegetation, J. Air Pollut. Control Assoc., 27, 1110–1116, https://doi.org/10.1080/00022470.1977.10470534, 1977.

Wiman, B. L. B. and Ågren, G. I.: Aerosol depletion and deposition in forests—A model analysis, Atmospheric Environ. 1967, 19, 335–347, https://doi.org/10.1016/0004-6981(85)90101-5, 1985.

Xiu, A. and Pleim, J. E.: Development of a Land Surface Model. Part I: Application in a Mesoscale Meteorological Model, J. Appl. Meteorol., 40, 192–209, https://doi.org/10.1175/1520-0450(2001)040<0192:DOALSM>2.0.CO;2, 2001.

Zhang, L., Gong, S., Padro, J., and Barrie, L.: A size-segregated particle dry deposition scheme for an atmospheric aerosol module, Atmos. Environ., 35, 549–560, https://doi.org/10.1016/S1352-2310(00)00326-5, 2001.

https://doi.org/10.5194/gmd-2021-129
Preprint. Discussion started: 17 May 2021

Geoscientific Model Development
Open Access
Discussions

Table 1. Detailed mechanistic equations used for different deposition schemes in this study.

					Single Diameter					Modal approach	Sectional approach
CTM	Scheme	V_d	V_g	R_a	Rs or R_b	E_B	E_{IM}	E_{IN}	St		
CAMx	Z01	$V_g + \frac{1}{R_a + R_s}$	$\frac{\rho d_p^2 g C}{18\eta}$	$\frac{\ln\left(\frac{Z_R}{Z_0}\right) - \Psi_H}{\kappa u_\star}$	$\frac{1}{\varepsilon_0 u_\star (E_B + E_{IM} + E_{IN}) R_1}$	$Sc^{-\gamma}$	$\left(\frac{S_t}{\alpha + S_t}\right)^{\beta}$	$\frac{1}{2}\left(\frac{d_p}{A}\right)^2$	$St = \frac{V_g u_\star}{gA}$	*Not applicable*	*Yes*
CMAQ	PR11	$\frac{V_g}{1 - e^{-V_g(R_a + R_b)}}$	$\frac{\rho d_p^2 g C}{18\eta}$	$0.95\frac{\ln\left(\frac{Z_R}{Z_0}\right) - \Psi_H}{\kappa u_\star}$	$\frac{1}{(1 + 0.24\frac{w_\star^2}{u_\star^2})u_\star(E_B + E_{IM} + E_{IN})}$	$Sc^{-\frac{2}{3}}$	$\left(\frac{St^2}{400 + St^2}\right)$	Not applicable, assume 0	$St = \frac{V_g u_\star^2}{g\nu}$	$\widehat{D}, \widehat{V_g}, \widehat{E_{IM}}$ $E_{IM} = \frac{St^2}{400}$	*Yes*
CMAQ	OFF	$\frac{V_g}{1 - e^{-V_g(R_a + R_b)}}$	$\frac{\rho d_p^2 g C}{18\eta}$	$0.95\frac{\ln\left(\frac{Z_R}{Z_0}\right) - \Psi_H}{\kappa u_\star}$	$\frac{1}{(1 + 0.24\frac{w_\star^2}{u_\star^2})u_\star(E_B + E_{IM} + E_{IN})}$	$Sc^{-\frac{2}{3}}$	$\left(\frac{St^2}{400 + St^2}\right)$	Not applicable, assume 0	$St = \frac{V_g u_\star^2}{g\nu}$	$\widehat{D}, \widehat{V_g}$	*Yes*
CMAQ	VGLAI	$\frac{V_g}{1 - e^{-V_g(R_a + R_b)}}$	$\frac{\rho d_p^2 g C}{18\eta}$	$0.95\frac{\ln\left(\frac{Z_R}{Z_0}\right) - \Psi_H}{\kappa u_\star}$	$\frac{1}{\{(1 + f_{veg}(lai - 1)) + 0.24\frac{w_\star^2}{u_\star^2})\}u_\star(E_B + E_{IM} + E_{IN})}$	$Sc^{-\frac{2}{3}}$	$\frac{St^2}{(1 + St^2)}$	Not applicable, assume 0	$St = \frac{V_g u_\star}{gA}$	$\widehat{D}, \widehat{V_g}, \widehat{E_{IM}}$ $\widehat{E_{IM}} = \frac{\widehat{St}^2}{\left(1 + \widehat{St}^2\right)}$ $\widehat{St} = \frac{\widehat{V_g} u_\star}{gA}$	*Yes*

https://doi.org/10.5194/gmd-2021-129
Preprint. Discussion started: 17 May 2021

Geoscientific Model Development
Discussions
Open Access
EGU

Table 2. Site information and required parameters to run DepoBoxToolv1.0.

Measurement study	Vong et al. (2004)	Lamaud et al. (1994)	Matsuda et al. (2010)
LUC	Grass	Coniferous forest	Deciduous forest
Size distribution	Number	Number	Volume
Sampling date	May-June 2000	June 1992	July 2009
Location	US	France	Japan
Latitude	44.46°N	44.84°N	36.40°N
Longitude	123.11°W	0.58°W	138.58°E
Density (ρ, kg/m3)	1500.00	1500.00	1500.00
Geometric mean diameter ($d_{pg}, \mu m$)	0.52	0.04	0.48
Geometric standard deviation (σ_g)	1.7 and 2.5	2.5	1.7 and 2.5
Temperature (K)	298.15	290.15	289.45
Pressure (pascal)	101325.00	101325.00	101325.00
Relative humidity (RH, %)	72.17	90.00	90.00
Leaf area index (LAI)	4.00	6.00	6.00
Horizontal wind speed (Uh, m/s)	2.18	3.53	1.30
Friction velocity (u_*, m/s)	0.18	0.60	0.20
Canopy height (h, m)	0.88	15.00	20.00
Zero-plane displacement height (d, m)	0.66	11.00	12.00
Roughness height (z0, m)	0.03	1.20	1.50
Measurement height (z, m)	5.00	25.00	27.00
Monin-Obukhov length (L0, m)	0.61	-10	-1.125
Convective velocity scale (w_*)	0.35	2.00	2.10

Note: all parameters are represented as median values.

https://doi.org/10.5194/gmd-2021-129
Preprint. Discussion started: 17 May 2021

Geoscientific Model Development Discussions
Open Access

Table 3. Results of the fractional biases for three land-use categories.

Incorporation	Scheme		Grass	Coniferous forest		Deciduous Forest
Single	Z01		-1.22	0.35		-1.42
	PR11, OFF		-1.45	-0.70		-1.79
	VGLAI		-1.27	0.37		-1.53
		σ_g=1.7	σ_g=2.5	σ_g=2.5	σ_g=1.7	σ_g=2.5
Sectional	Z01	-1.19	-1.10	0.5	-1.52	0.92
	PR11, OFF	-1.40	-1.24	-0.52	-1.76	1.21
	VGLAI	-1.23	-1.09	0.55	-1.64	1.03
Modal	PR11	-1.40	-1.19	-0.45	-1.77	1.67
	OFF	-1.40	-1.25	-0.45	-1.79	0.69
	VGLAI	-1.21	-1.07	0.62	-1.64	1.16

https://doi.org/10.5194/gmd-2021-129
Preprint. Discussion started: 17 May 2021

Geoscientific Model Development
Discussions

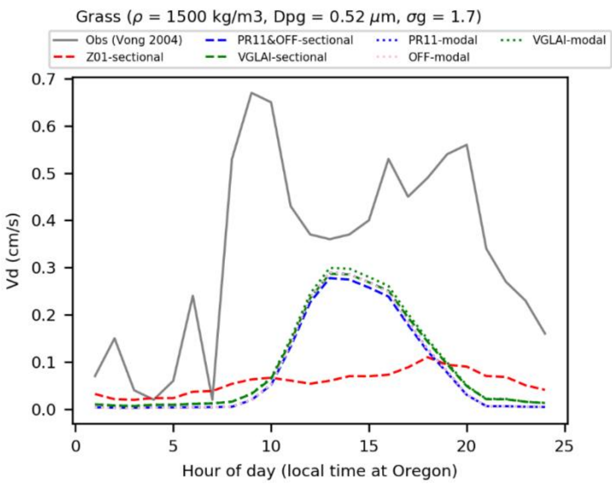

A

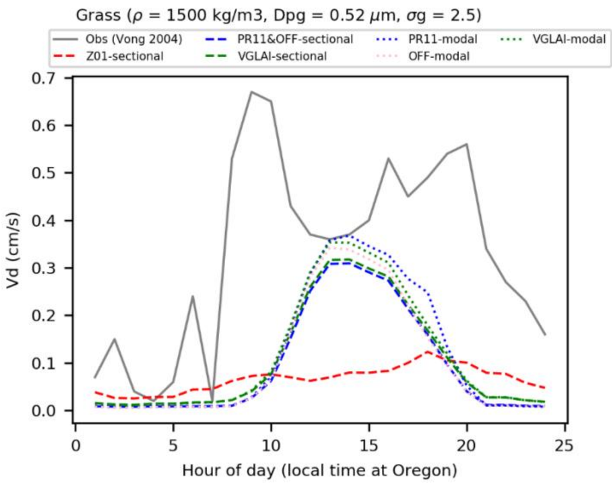

B

Fig. 1. Diurnal variations of instantaneous hourly V_d on grass based on particle number. A) σ_g = 1.7 , B) σ_g = 2.5. σ_g was not reported in measurement so two values commonly found in CMAQ were assumed. Because PR11 and OFF share the same mechanistic dry deposition scheme and predict the same results for the sectional approach, they are presented together. For the modal approach, PR11 includes the impaction integration while OFF excludes the impaction integration factor. They are thus presented separately.

https://doi.org/10.5194/gmd-2021-129
Preprint. Discussion started: 17 May 2021

Geoscientific Model Development
Discussions

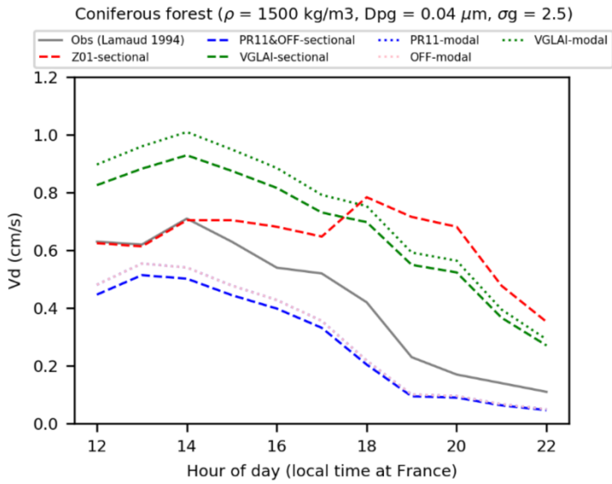

Fig. 2. Diurnal variations of instantaneous hourly V_d on coniferous forest based on particle number. σ_g = 2.5 was reported in the measurement study. The legend corresponds to that of Fig. 1.

https://doi.org/10.5194/gmd-2021-129
Preprint. Discussion started: 17 May 2021

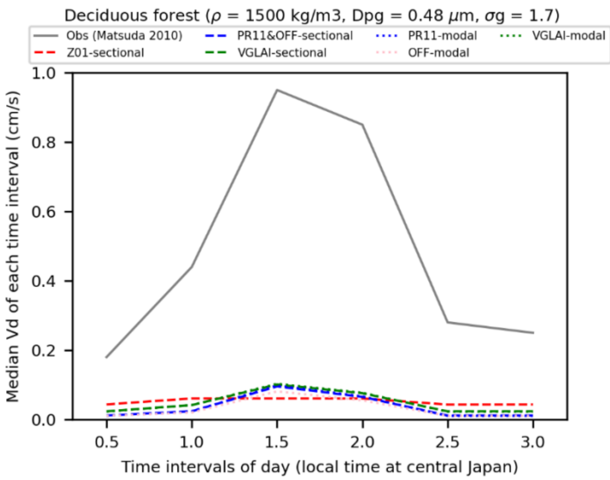

A

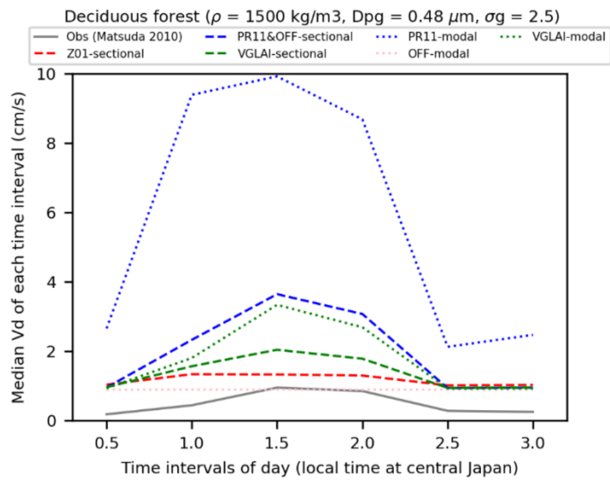

B

Fig. 3. Diurnal variations of median V_d on deciduous forest based on particle volumes. A) σ_g = 1.7, B) σ_g = 2.5. Since σ_g was not reported in the measurements, two values typical of background aerosol were assumed. The legend corresponds to that of Fig. 1.

https://doi.org/10.5194/gmd-2021-129
Preprint. Discussion started: 17 May 2021

Geoscientific Model Development
Discussions

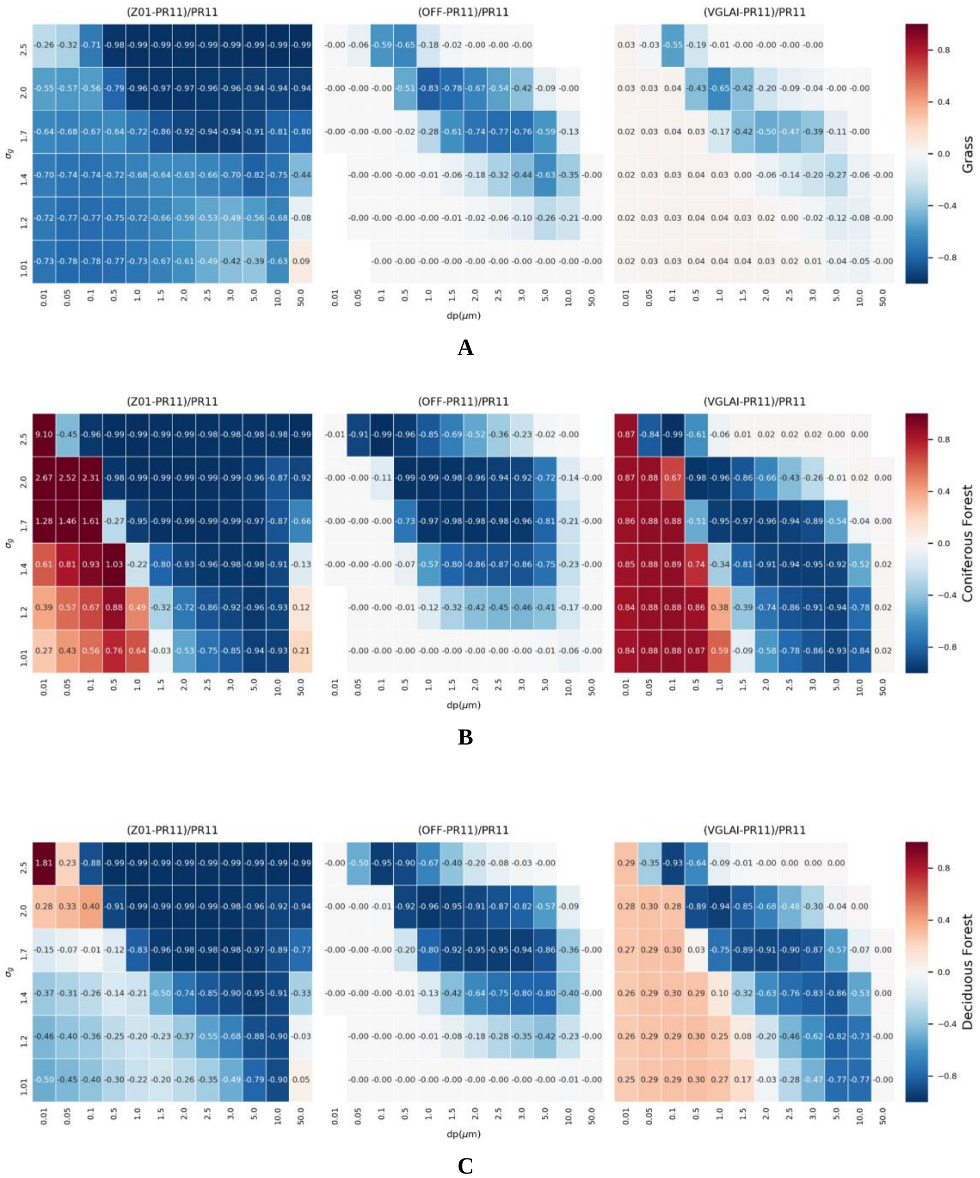

Fig. 4. Sensitivity analysis of deposition velocity to σ_g and d_p on different land-use types. A) grass, B) coniferous and C) deciduous forest

https://doi.org/10.5194/gmd-2021-129
Preprint. Discussion started: 17 May 2021

Geoscientific Model Development
Open Access
Discussions

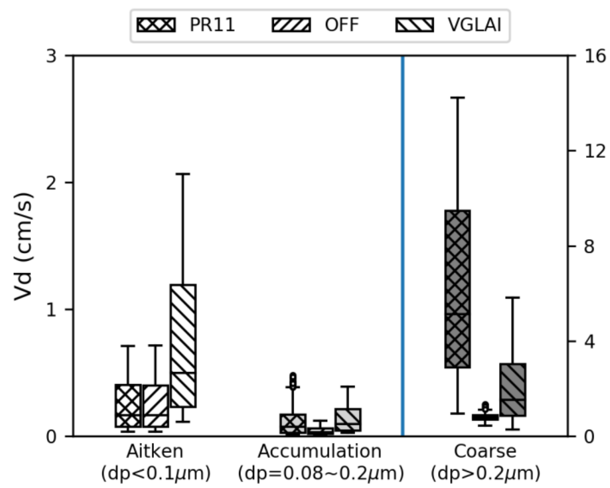

A

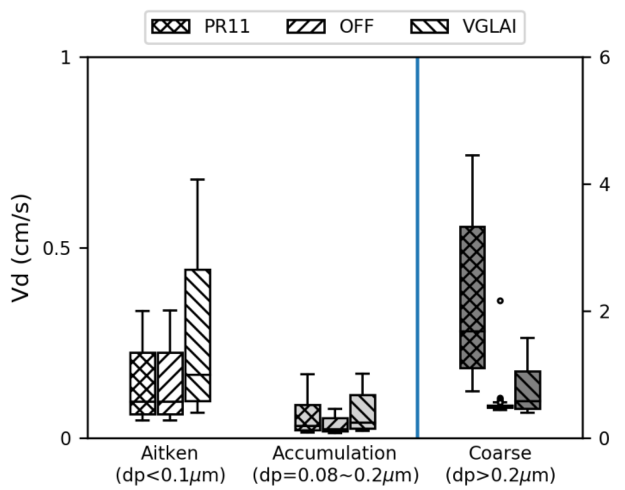

B

Fig. 5. Box plot of spatially averaged hourly dry deposition velocities for a A) forested and B) non-forested surface modeled in July for three types of particle sizes in CMAQ.

https://doi.org/10.5194/gmd-2021-129
Preprint. Discussion started: 17 May 2021

Geoscientific Model Development Discussions
Open Access

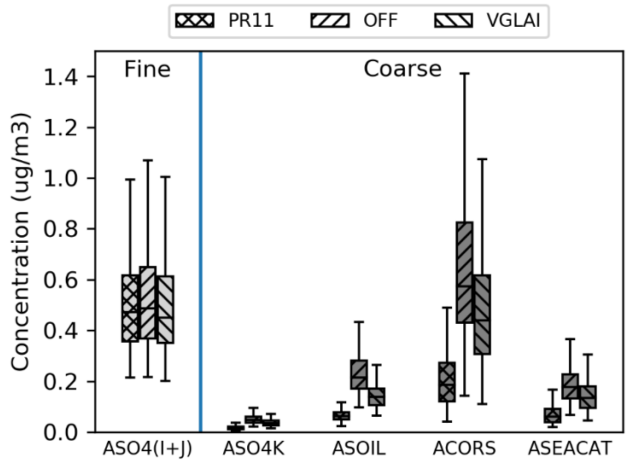

A

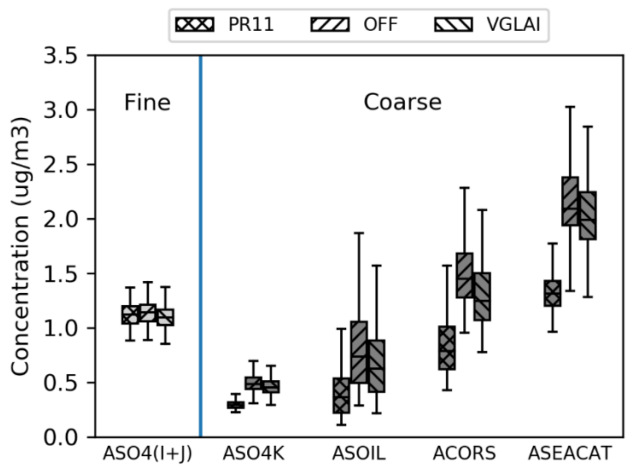

B

Fig. 6. Box plot of spatially averaged hourly concentrations above a A) forested and B) non-forested surface in July for a selection of single-compound and lumped species in CMAQ.

5

https://doi.org/10.5194/gmd-2021-129
Preprint. Discussion started: 17 May 2021

Geoscientific Model Development Discussions

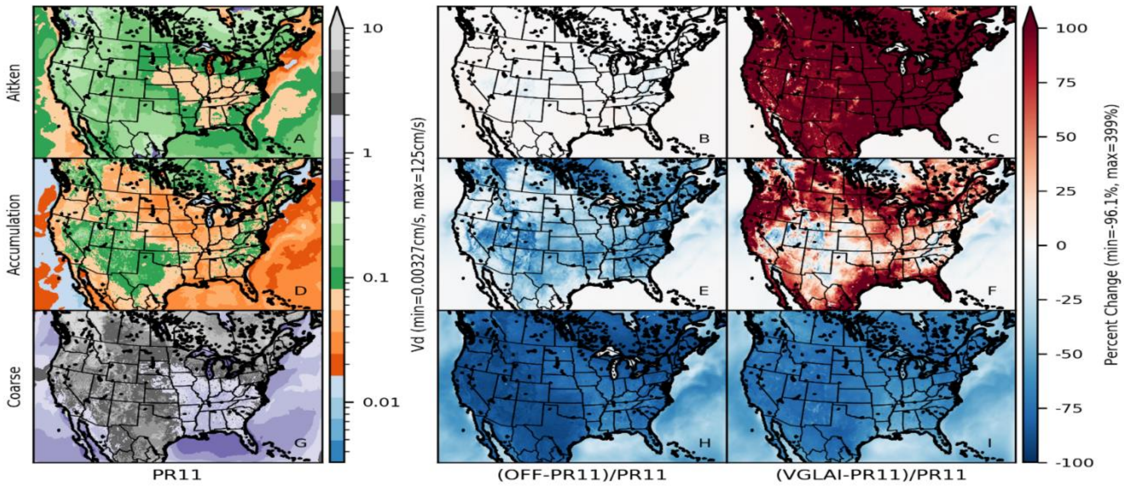

Fig. 7. Monthly mean SO_4 dry deposition velocity (cm/s) for PR11 at three size modes (A, D, G) and the corresponding percent changes with updated dry deposition schemes for OFF (B, E, H) and VGLAI (C, F, I) from a 12km grid resolution CMAQ simulation.

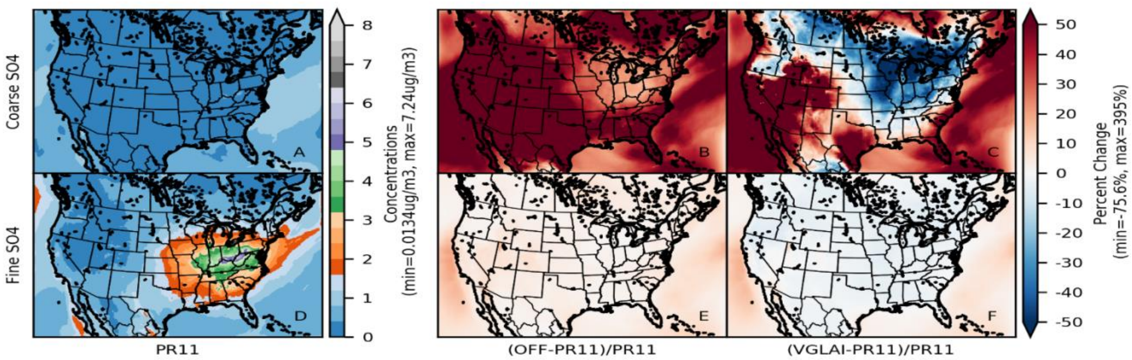

Fig. 8. Monthly mean coarse and fine SO_4 concentration (μg/m3) for PR11 (A, D) and the corresponding percent changes with updated dry deposition schemes for OFF (B, E) and VGLAI (C, F) from a 12 km grid resolution CMAQ simulation in July 2011.

https://doi.org/10.5194/gmd-2021-129
Preprint. Discussion started: 17 May 2021

Geoscientific Model Development
Discussions

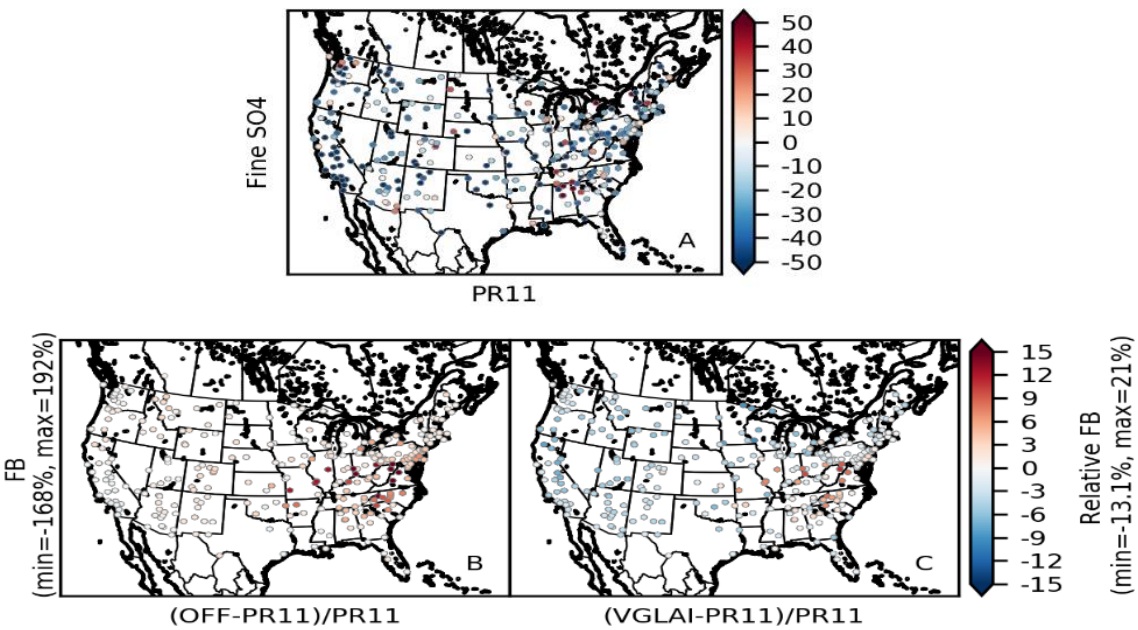

Fig. 9. Fractional Bias (F_B) of fine SO_4 for PR11 at IMPROVE and CSN sites (A) and the corresponding relative change of F_B between OFF and PR11 (B), and VGLAI and PR11 (C).